High-temperature shrinkage suppression in refractory ceramic fiber board using novel surface coating agent

Naoya Takahashi, Shinobu Hashimoto, Yusuke Daiko, Sawao Honda, Yuji Iwamoto

Department of Life Science and Applied Chemistry, Division of Advanced Ceramics, Nagoya Institute of Technology, Gokiso-cho, Showa-ku, Nagoya 466-8555, JAPAN

Keywords: Refractory, Ceramic fiber, Shrinkage, Coating, Compressive strength

Abstract

Refractory ceramic fiber (RCF) boards are widely used because their insulating properties allow them to reduce energy consumption during high-temperature industrial processes. However, since conventional RCF boards undergo a linear shrinkage of more than 3% above 1300°C, furnace lining parts, such as the ceiling, wall, and bottom made of RCF board easily become fragile. In order to suppress the shrinkage of the RCF board above 1300°C, the RCF board surface was coated with a silica sol containing several types of alumina particles. When a RCF board coated with a silica sol slurry containing 50 mass% alumina platelets was heated at 1400°C for 8 h, the linear shrinkage of the RCF board decreased from 4.3% to 1.5%. This, in turn, improved the heat resistance of the RCF board up to 1400°C.

Corresponding author: n.takahashi.347@stn.nitech.ac.jp

1. Introduction

Refractory ceramic fiber (RCF) products such as boards and blankets are widely used in high-temperature industries, such as ceramics, metal refining, and glass and cement production [1]. However, RCFs are considered to be carcinogenic when inhaled, and the International Agency for Research on Cancer (IARC) has designated RCF as cancer risk category 2 [2-4]. The Japanese Ministry of Health, Labor and Welfare has also designated RCF as a cancer risk material in November 2015. Nonetheless, in Japan at present, RCF boards are not covered by these guidelines, since it is considered that processed industrial products made from RCF are unlikely to release fibers into the atmosphere. This is because, before any cutting or grinding of RCF boards is performed, the boards are pre-treated, usually by dipping them in a silica sol solution, which dramatically decreases the amount of fiber scattering. Upon heating, linear shrinkage of RCF boards coated with silica sol tends to increase relative to that for untreated RCF boards. The devitrification (crystallization) and subsequent shrinkage observed during the use of RCF boards are critical problems because they result in spalling of the furnace lining [5-10]. Numerous techniques for coating metal and ceramic parts with ceramic have been studied to increase the heat and/or corrosion resistance [11-18]. In the case of RCF boards, attempts have been made to improve the thermal resistivity by varying the chemical composition [19-21]. However, sol solution coating, which reduces the shrinkage of RCF boards during heating, has not been studied to date.

To reduce the heat-induced shrinkage of RCF boards, a novel coating agent consisting of several types of alumina particles and a standard silica sol solution was prepared. In the present study, the effect of this new coating method on the linear shrinkage after heating was investigated. Changes with temperature in the reaction

products and the microstructure of the RCF board after this coating treatment were studied. In addition, the change in the compressive strength of the RCF board with heat treatment was examined. Furthermore, to clarify the shrinkage suppression mechanism for RCF boards with the proposed coating agent, the thermal expansion behavior of a pre-cast sample of the coating layer alone was investigated.

2. Experimental

A commercial product manufactured by ITM Co. Ltd. (Japan) was used as a refractory ceramic fiber (RCF) board. The chemical compositions of the RCF board and the silica sol solution used in this study are presented in **Tables 1 and 2**, respectively. The fiber diameters in the RCF board were mostly in the 2-4 μm range. The properties of the alumina particles mixed with the silica sol solution to form a coating slurry are listed in **Table 3**. All alumina particles were reagent grade. The coating slurry was made from a silica sol solution and different types of alumina particles mixed with various ratios.

First, the RCF board was cut into rectangular (25×25×50 mm) test pieces. Then, each test piece was immersed in the coating slurry for several seconds. In order to investigate the coating state of the RCF test piece after coating treatment, the test piece was analyzed by X-ray tomography (inspeXio SMX-225CT, SHIMADZU, Japan). The test piece subjected to coating treatment was dried for 1 day at room temperature, then heated at a fixed temperature for 8 h. The heating rate was 5°C/min. The linear shrinkage of the test piece induced by heating at a fixed temperature was measured at room temperature. The changes in the crystalline phases and microstructure of the surface and interior of the heated test piece were analyzed by X-ray diffraction (XRD;

X'Pert MPD, Panalytical, Netherlands) and scanning electron microscopy (SEM; S-2360N, HITACHI, Japan).

To clarify the shrinkage suppression mechanism for the RCF board with coating treatment during heating, the compressive strength of the test piece with coating treatment after heating at various temperatures was examined (crosshead speed: 0.5 mm/min). Furthermore, the coating slurry was cast into a gypsum mold by itself, kept for 12 h and dried at 105°C for 24 h to form a hardened body. This sample was cut into 5×5×10 mm test pieces, parallel and perpendicular to the direction along which the platelets were arranged, for thermal expansion measurements. These measurements were made during heating to 1300°C at a rate of 5°C/min and maintaining that temperature.

3. Results and discussion

3.1 Linear shrinkage of RCF board with and without slurry treatment

First, an immersion slurry was prepared from 50% silica sol and 50% alumina particles of one type. **Figure 1** shows the changes in the linear shrinkage of the RCF board with and without an alumina-particle-containing slurry with heat treatment temperature. As a reference, when the silica sol was used alone as an immersion slurry, the linear shrinkage of the RCF board was larger than in the case of a standard RCF board at temperatures above 1100°C. The reason for this will be discussed below on the basis of crystal changes in the RCF board with and without silica sol slurry after heating. By contrast, when the RCF board was immersed in the slurry with alumina particles, the linear shrinkage of the RCF boards was either larger or smaller than that for a standard RCF board after heating. When a slurry with 0.5-μm alumina particles was

used, no suppression was observed in the linear shrinkage of the RCF board above 1200°C: the shrinkage was the same as that of the silica sol coating itself. With increasing alumina particle size, suppression in the linear shrinkage of the RCF board was observed: when a slurry with alumina particles having an average size of 4.5 μm was used, the linear shrinkage of the RCF board after heating at 1000-1400°C decreased to the level observed for a RCF board immersed in a slurry with 1.0-μm alumina particles. However, when a slurry with larger (50 μm) alumina particles was used, the coating layer became too thick and nonuniform. Hence, 4.5 μm was concluded to be the ideal alumina particle size for the RCF board coating slurry.

Anisotropic alumina platelets, 7-10 μm in diameter, were used as alumina particles, resulting in a uniform slurry coating on the RCF board, and the linear shrinkage decreased after heating at 1200-1400°C relative to the RCF board with a 4.5-μm alumina particle slurry. Clearly, the slurry with alumina platelets had the largest suppression effect on the linear shrinkage of the RCF board.

So far, only slurries consisting of silica sol and alumina particles in equal weight were used. To determine the optimal ratio of silica sol to alumina platelets for achieving the lowest linear shrinkage rate for RCF boards after heating, slurries with various ratios of silica sol to alumina particles were prepared. **Figure 2** shows the variations in linear shrinkage rate of the RCF board for various ratios and two kinds of alumina particles (particles with 4.5-μm average diameter and platelets) after heating at 1400°C for 8 h. For all ratios of silica sol to alumina particles, when platelets were used, the linear shrinkage rate of the RCF board was lower than that for the RCF board with 4.5-μm alumina particles. In addition, the linear shrinkage for the RCF board decreased with increasing amount of alumina platelets up to 50 wt%, where the lowest shrinkage

of this study was observed. However, when a slurry with 70 wt% alumina platelets was used, the linear shrinkage for the RCF board increased. By contrast, when 4.5-μm alumina particles were used, the linear shrinkage was the lowest at 70 wt%. The optimum amount of alumina particles for the suppression of linear shrinkage seemed to vary with the shape of the alumina particles. When a slurry with a larger amount of alumina platelets, e.g., 70 wt%, was used, the amount of silica sol was too small to obtain the lowest linear shrinkage for the RCF board. Thus, alumina platelets were selected and fixed at 50 wt% to prepare the RCF coating slurry in the following experiments.

3.2 State and microstructure of alumina-platelet-containing coating slurry for RCF board

After immersion treatment with the slurry before heating, the slurry distribution inside the RCF board was not clear. In order to observe the state of the RCF board after slurry immersion treatment, X-ray tomography was performed. **Figure 3** shows X-ray tomography images of RCF boards with no coating (normal), with a purely silica sol slurry and with a slurry containing alumina platelets, before heating. In these images, the distribution of both the purely silica sol slurry and the slurry with alumina platelets shows up white, since the dense part of the RCF board with slurry prevented the transmission of X-rays. When the silica-sol-only slurry was used, the silica sol was distributed near the surface, in a layer approximately 2 mm in thickness. However, the fact that the white region corresponding to the silica sol was not uniform suggested that the silica sol distribution at the surface of the RCF board was not uniform. By contrast, when the slurry with alumina platelets was used, a white surface layer approximately 300-400 μm in thickness was observed. Since the slurry with alumina platelets did not

infiltrate the RCF board, a uniform coating layer could be formed at the surface of the RCF board.

Figure 4 shows SEM images of the cross-section of the RCF board with alumina-platelets-containing slurry before heating. The alumina platelets were stacked up on the RCF board surface. An intermediate layer consisted of alumina platelets and fibers was also observed. However, since the location of the silica sol could not be confirmed, the silica sol seemed to spread on the surface of the platelets and bind them to each other. However, the actual mechanism of shrinkage suppression of the RCF board with alumina-platelet-containing slurry after heating was not clear. The following section will discuss the variation with temperature of the physicochemical properties of the RCF board with alumina-platelet-containing slurry, such as the ~~crystal~~ crystalline phase, microstructure, and compressive strength. In addition, the thermal expansion behavior of the silica-sol-only slurry with heating temperature was investigated.

3.3 Changes with temperature of crystalline phase of slurry with alumina platelets

Figure 5 shows the changes of crystalline phases of the coating layer of the RCF board with alumina-platelet-containing slurry and the interior of the RCF board without coating. As a reference, XRD patterns for the crystalline phases of the purely-silica-sol case after heating are also shown. Both the starting silica sol and the RCF board showed only a broad peak, suggesting that they consisted of an amorphous phase. When the RCF board was heated at 1100°C, mullite was detected in the amorphous aluminosilicate fibers. After heating at 1300°C, cristobalite was also detected. By contrast, in the coating layer, cristobalite derived from the silica sol was detected at 1100°C. The increase in the shrinkage of the RCF board with the silica-sol-only slurry was thought to be caused by

this lower-temperature crystallization to cristobalite, as shown in Fig. 1. Since upon heating the silica-sol-only slurry at 1300°C the cristobalite diffraction peaks increased and their intensities were the same as those for the coating layer at 1500°C, most of the amorphous silica sol of the coating presumably changed completely into the crystalline cristobalite phase at 1300°C. When the coating layer was heated at 1400°C, the crystalline phases did not change relative to those of the coating layer after heating at 1300°C. Upon heating the coating layer at 1500°C, the cristobalite peaks disappeared, while mullite was detected. This mullite was presumably formed by the reaction between the cristobalite derived from silica sol and alumina platelets.

3.4 Changes with temperature of compressive strength of the RCF board with alumina-platelet-containing slurry

The compressive strength of RCF boards with and without slurry coating treatment was investigated. **Figure 6** shows the compressive strength of the original (untreated) RCF board and RCF boards with purely silica sol slurry or alumina-platelet-containing slurry after heating. When the original RCF board was heated at 1300°C, the compressive strength of the board was approximately 0.07 MPa. Upon silica-sol-only coating, the compressive strength of the RCF board exceeded 0.22 MPa after heating at 1300°C, although the linear shrinkage of the RCF board was larger than that of the original RCF board. The amorphous silica sol that infiltrated into the spaces between the fibers around the surface transformed into cristobalite, which promoted the linear shrinkage, thought to increase the compressive strength. By contrast, when the slurry with alumina platelets was used, the alumina platelets stacked up into a 300-400-μm layer on the surface of the RCF board and cristobalite crystals formed between the

platelets, connecting the platelets and increasing the mechanical strength of the coating layer. This increased the compressive strength of the RCF board. Upon heating at 1300°C, the pure-silica-sol-derived gel transformed into cristobalite, leading to a maximum compressive strength of 0.67 MPa for the RCF board. Thus, the coating treatment using the slurry for the RCF board increased the compressive strength by a factor of about 10. However, with heating at 1400°C, the compressive strength of the RCF board decreased to 0.55 MPa, although the crystalline phases did not change compared to the result for the coating layer of the RCF board at 1300°C. Therefore, the microstructure of the coating layer of the RCF board was characterized.

Figure 7 shows SEM micrographs of the surface of RCF boards coated with the alumina platelet slurry after heating at 1100-1400°C. Upon heating at 1100 and 1300°C, each alumina platelet could be distinguished. By contrast, when the RCF board coated with the alumina platelet slurry was heated at 1400°C, the alumina platelets in the coating layer seemed to coalesce. The resulting microstructure was indicative of increased mechanical strength. In fact, the compressive strength of the RCF board coated with alumina platelet slurry decreased relative to that of a plain RCF board at 1300°C, as shown in Fig. 6. According to Fig. 5, upon heating the RCF board at 1500°C, cristobalite reacted completely with the alumina platelets to form mullite. Thus, when the RCF board with alumina platelet slurry was heated at 1400°C, the mechanical strength presumably decreased.

Figure 8 shows the changes of stress-displacement curves of the RCF board with alumina-platelet-containing slurry with and without heat treatment. In the case of the RCF board with heating at 1300°C, the curve behavior was not a liner proportional relationship which caused to increase its compressive strength. On the contrary, with

heating at 1400°C, the curve had a tendency of liner proportion which was a brittle behavior. Hence the compressive strength of the RCF board is thought to be decreased.

3.5 Shrinkage suppression mechanism for RCF board using alumina platelet coating slurry

On the basis of the compressive strength, the microstructure and ~~crystal~~ crystalline phases of the RCF board coated with alumina platelet-containing slurry after heating, the shrinkage suppression mechanism for the RCF board was considered to be as follows. Figure 5 clearly shows that the XRD peak intensities associated with cristobalite increased, owing to the increase in the crystallinity and/or content of cristobalite, leading to a high compressive strength in the case of the RCF board coated with slurry. However, the reason why the coating layer consisting of alumina platelets and cristobalite showed shrinkage suppression after heating at high temperature was unclear. Hence, a pre-cast sample consisting of alumina platelets and silica sol was prepared. **Figure 9** shows the thermal expansion behavior of the pre-cast sample consisting of 50 wt% silica sol and 50 wt% alumina platelets along two directions: parallel and perpendicular to the platelet orientation during heating to, and maintaining at, 1300°C. In the perpendicular direction, after heating at 1300°C for 120 min, the shrinkage reached 1.7%. By contrast, in the parallel direction, no shrinkage occurred up to 1300°C. This directional shrinkage behavior was thought to be identical to that for the shrinkage of the coating layer. In fact, according to Fig. 1, since the original RCF board showed a shrinkage of 4.5% at 1300°C, the linear shrinkage of the RCF board with the alumina platelet slurry was 1.5% at 1300°C.

On the basis of the above results, **Figure 10** shows the shrinkage suppression

mechanism for the RCF board with alumina platelet slurry during heating. A standard uncoated RCF board would shrink markedly during heating, owing to the crystallization of the fibers to cristobalite with bending behavior. However, when a RCF board coated with a slurry containing alumina platelets was heated, since the coating became a hard shell consisting of alumina platelets and cristobalite at above 1100°C (mullite, $3Al_2O_3 \cdot 2SiO_2$, precipitates at 1500°C), coating the RCF board, the RCF board with slurry showed a higher mechanical strength and lower linear shrinkage than the original RCF board. Given the applicability of this coating technique, other fiber industrial products such as alkaline earth silicates (AES; such as bio soluble fibers) would be expected to be usable at temperatures above the conventional temperature limit.

4. Summary

In order to decrease the linear shrinkage of the RCF board during heating, a novel coating consisting of silica sol and alumina particles was developed. Most effective in suppressing linear shrinkage was the coating slurry consisting of silica sol and alumina platelets. When the RCF board was coated with a slurry consisting of 50 wt% silica sol and 50 wt% alumina platelets, the linear shrinkage was 1.5% at 1400°C. Upon heating at 1100°C, the silica sol began to transform into cristobalite and the reaction was completed at 1300°C. Thus, the compressive strength of the RCF board with and without slurry was 0.07 MPa and 0.67 MPa after heating at 1300°C, respectively. That is, the slurry coating treatment increased the compressive strength of the RCF board by about 10 times. Furthermore, since this hard, shell-like (thickness: 300-400 μm) coating on the RCF board exhibited low linear shrinkage and thus prevented the RCF board from shrinking, the linear shrinkage of the RCF board improved from 4.3% to 1.5% upon

application of the alumina platelet slurry. This coating technique is expected to be applicable to other fiber products, such as AES fibers.

References

[1] V.F. Shishkin, K.M. Mikhalev, Increase in the operating efficiency of heating units using ceramic fibers and objects based on them, Refract. Ind. Ceram. 50 (2009) 313-318

[2] R.W. Mast, E.E. McConnell, R. Anderson, J. Chevalier, P. Kotin, D.M. Bernstein, P. Thevenaz, L.R. Glass, W.C. Miller, Studies on the chronic toxicity (inhalation) of four types of refractory ceramic fiber in male Fischer 344 rats, Inhal. Toxicol. 7 (1995) 425-467

[3] J. Lockey, G. Lemasters, C. Rice, K. Hansen, L. Levin, R. Shipley, H. Spitz, J. Wiot, Refractory ceramic fiber exposure and pleural plaques, Am. J. Respir. Crit. Care Medicine 154 (1996) 1405-1410

[4] L.D. Maxim, M.J. Utell, Review of refractory ceramic fiber (RCF) toxicity, epidemiology and occupational exposure, Inhal. Toxicol. 30 (2018) 49-71

[5] B.A. Scowcroft, G.C. Padgett, The structure and thermal behaviour of ceramic fible blankets, Trans. Br. Ceram. 72 (1973) 11-14

[6] J.M. Curtis, Devitrification and shrinkage of alumina-silica based refractory insulating fibers, Master thesis, Colorado School of Mines (1993)

[7] É.V. Degtyareva, V.V. Martynenko, A.N. Gadou. E.I. Zoz, Reduction of linear shrinkage in glass-fiber refractories during service, Refractories 24 (1983) 3-7

[8] A.K. Bhattacharyya, B.N. Choudhury, P. Chintaiah, P. Das, Studies on a probable correlation between thermal conductivity, kinetics of devitrification and changes in fiber radius of an aluminosilicate ceramic vitreous fiber on heat treatment, Ceram. Int. 28

(2002) 711-717

[9] T.P. Brown, Paul T.C. Harrison, Crystalline silica in heated man-made vitreous fibres, Regul. Toxicol. Pharmacol. 68 (2014) 152–159

[10] D.J. Pysher, K.C. Goretta, R.S. Hodder Jr., R.E. Tressler, Strengths of Ceramic Fibers at Elevated Temperatures, J. Am. Ceram. Soc. 72 (1989) 284-288

[11] X.Q. Cao, R. Vassen, D. Stoever, Ceramic materials for thermal barrier coatings, J. Eur. Ceram. Soc., 24 (2004) 1-10

[12] M. Herrmann, F.-L. Toma, L.-M. Berger, G. Kaiser, C.C. Stahr, Comparative study of the corrosion resistance of thermally sprayed ceramic coatings and their bulk ceramic counterparts, J. Eur. Ceram. Soc., 34 (2014) 493-504

[13] S. Li, X. Zhao, G. Hou, W. Deng, Y. An, H. Zhou, J. Chen, Thermomechanical properties and thermal cycle resistance of plasma-sprayed mullite coating and mullite/zirconia composite coatings, Ceram. Int. 42 (2016) 17447-17455

[14] D. Liu, P. Hu, G. Chen, W. Han, Fabrication of silicon carbide coating on mullite fiber-reinforced mullite matrix composite via dip-coating, Ceram. Int. 44 (2018) 2584-2586

[15] Y. Zhang, H. Wang, T. Li, Y. Fu, J. Ren, Ultra-high temperature ceramic coating for carbon/carbon composites against ablation above 2000K, Ceram. Int. 44 (2018) 3056-3063

[16] N. Liao, Y. Li, J. Shan, T. Zhu, S. Sang, D. Jia, Improved oxidation resistance of expanded graphite through nano SiC coating, Ceram. Int. 44 (2018) 3319-3325

[17] M.A. Zavareh, A.A.D. M. Sarhan, R. Karimzadeh, R.S.A./l.K. Singh, Analysis of corrosion protection behavior of Al_2O_3-TiO_2 oxide ceramic coating on carbon steel pipes for petroleum industry, Ceram. Int. 44 (2018) 5967-5975

[18] M.D. Nguyen, J.W. Bang, Y.H. Kim, A.S. Bin, K.H. Hwang, V.-H. Pham, W.-T. Kwon, Slurry spray coating of carbon steel for use in oxidizing and humid environments, Ceram. Int. 44 (2018) 8306-8313

[19] H. Liu, X. Wang, B. Zhang, Z. Wang, Y. Yang, Structure and properties of CaO-MgO-SiO_2 Inorganic Glass Fiber with Additives (Al_2O_3, Y_2O_3), J. Wuhan Univ. Technol.-Mat. Sci. Ed. 27 (2012) 58-62

[20] L.E. Olds, W.C. Miller, J.M. Pallo, High temperature alumina-silicate fibers stabilized with Cr_2O_3, Am. Ceram. Soc. Bull. 59 (1980) 739-741

[21] M. Chatterjee, M.K. Naskar, P.K. Chakrabarty, D. Ganguli, Sol-gel alumina fibre mats for high-temperature applications, Mater. Lett. 57 (2002) 87-93

Figure and table captions

Figure 1 Linear shrinkage of RCF boards (uncoated or coated with various slurries) against heating temperature for 8 h.

Figure 2 Linear shrinkage rate of RCF boards versus the alumina content after heating at 1400°C for 8 h. Two kinds of alumina particles (round particles with an average diameter of 4.5 μm and platelets) were added to the silica sol.

Figure 3 X-ray tomographs of (a) uncoated RCF boards (normal), RCF boards coated with (a) silica sol only and (c) coating slurry containing alumina platelets before heating at 1300°C for 8 h.

Figure 4 SEM micrographs of the cross-section of the RCF board coated with the alumina-platelet-containing slurry before heating.

Figure 5 Changes in the ~~crystal~~ crystalline phases of the coating layer on the RCF board formed by applying an alumina-platelet-containing slurry and of the interior of an untreated RCF board.

Figure 6 Compressive strength of the original RCF board and of RCF boards with a silica-sol-only slurry or an alumina platelet slurry after heating.

Figure 7 SEM micrographs of the surface of RCF boards coated with an alumina platelet slurry, after heating at 1100-1400°C.

Figure 8 Changes of stress-displacement curves of the RCF board with alumina-platelet-containing slurry with and without heat treatment.

Figure 9 Thermal expansion behavior of pre-cast samples consisting of 50 wt% silica sol and 50 wt% alumina platelets along two directions: parallel and perpendicular to the platelet direction during heating and maintaining at 1300°C.

Figure 10 Shrinkage suppression mechanism for the RCF board with alumina-platelet-containing slurry during heating.

Table 1 Chemical composition of the RCF board used.

Table 2 Chemical composition of the silica sol solution used.

Table 3 Characteristics of the alumina particles used.

Figure 1

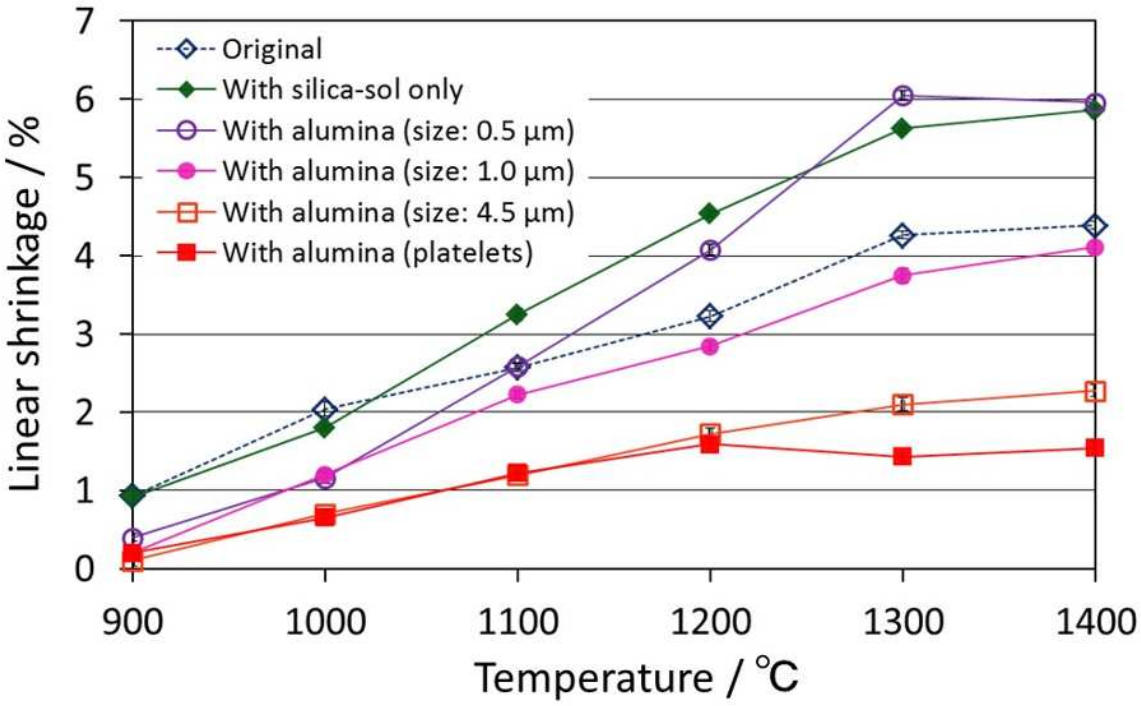
Original
With silica-sol only
With alumina (size: 0.5 µm)
With alumina (size: 1.0 µm)
With alumina (size: 4.5 µm)
With alumina (platelets)
Linear shrinkage / %
Temperature / °C
0
1
2
3
4
5
6
7
900
1000
1100
1200
1300
1400

Figure 2

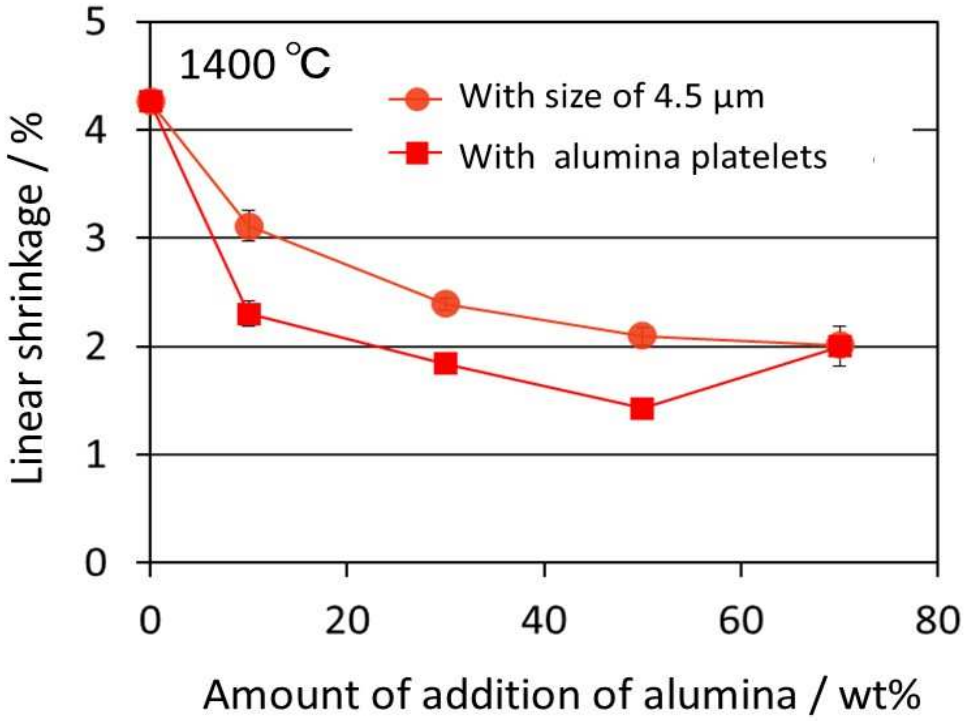
1400 °C
With size of 4.5 µm
With alumina platelets
Linear shrinkage / %
Amount of addition of alumina / wt%
0
1
2
3
4
5
0
20
40
60
80

Figure 3

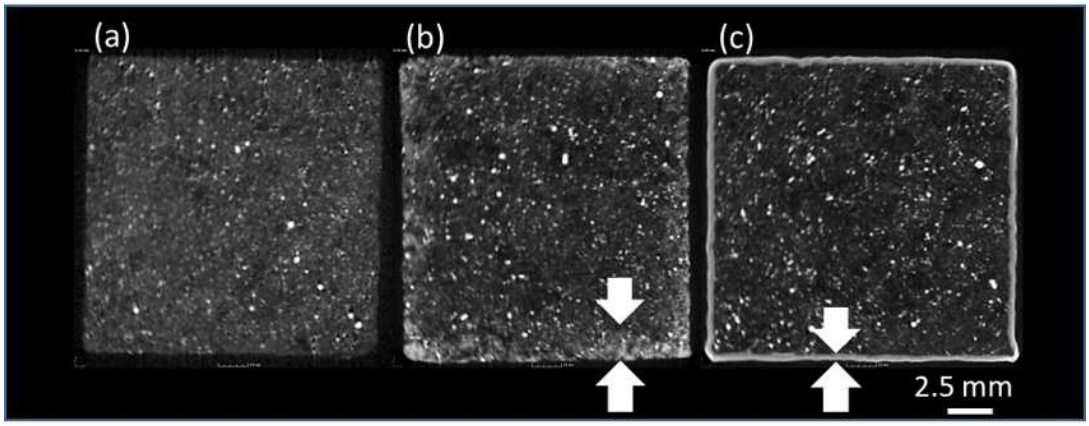

Figure 4

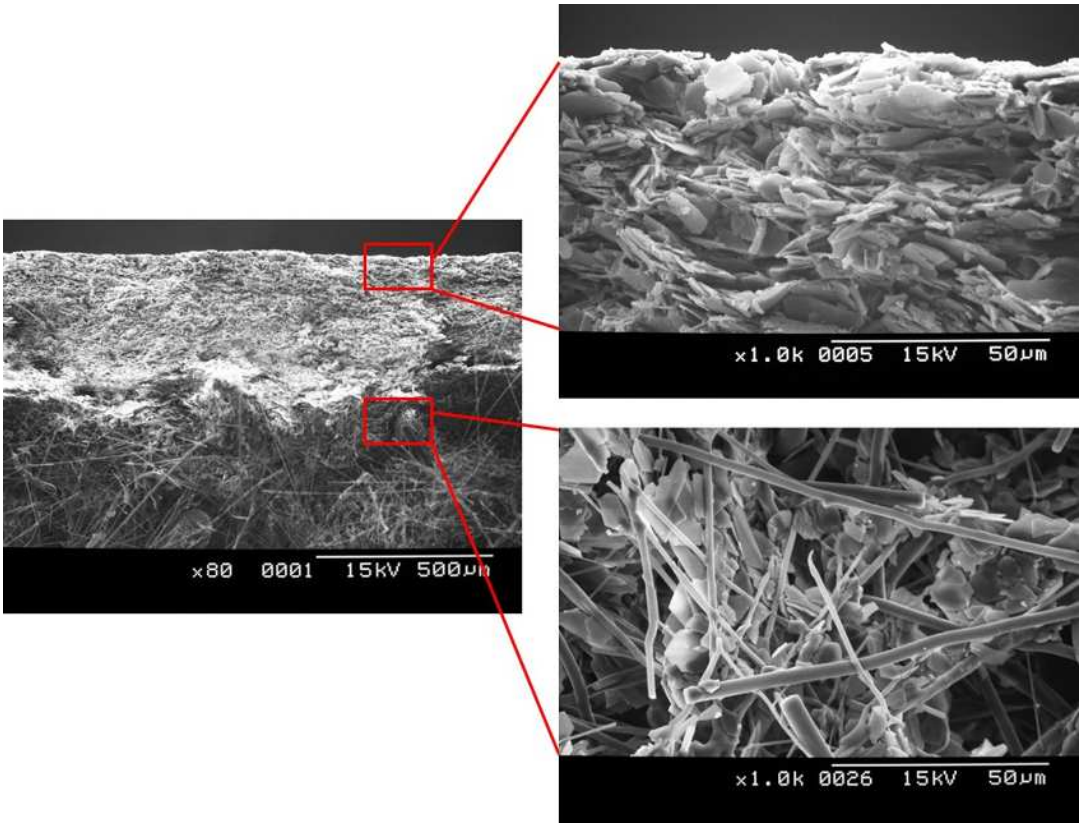

Figure 5

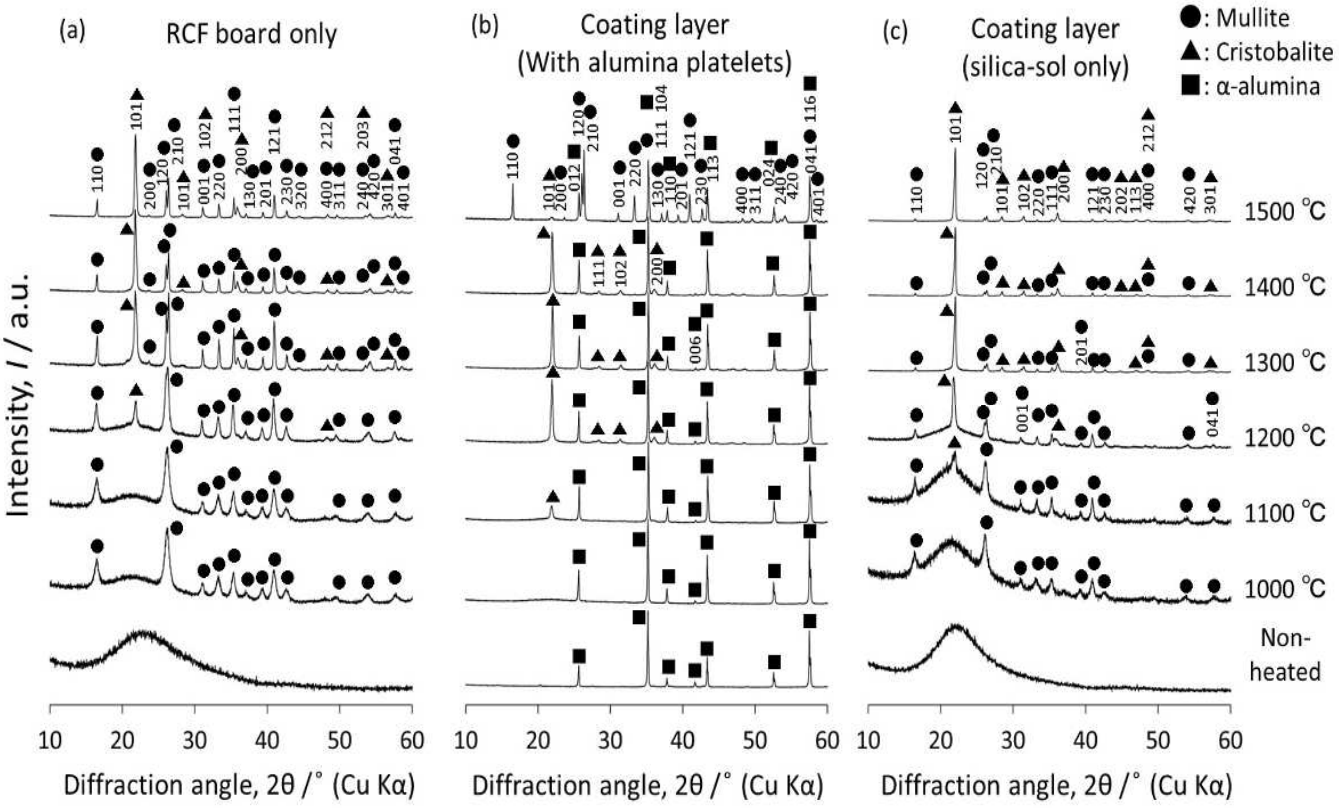
(a) RCF board only
(b) Coating layer (With alumina platelets)
(c) Coating layer (silica-sol only)
●: Mullite
▲: Cristobalite
■: α-alumina
1500 ℃
1400 ℃
1300 ℃
1200 ℃
1100 ℃
1000 ℃
Non-heated
Intensity, I / a.u.
Diffraction angle, 2θ /° (Cu Kα)
Diffraction angle, 2θ /° (Cu Kα)
Diffraction angle, 2θ /° (Cu Kα)

Figure 6

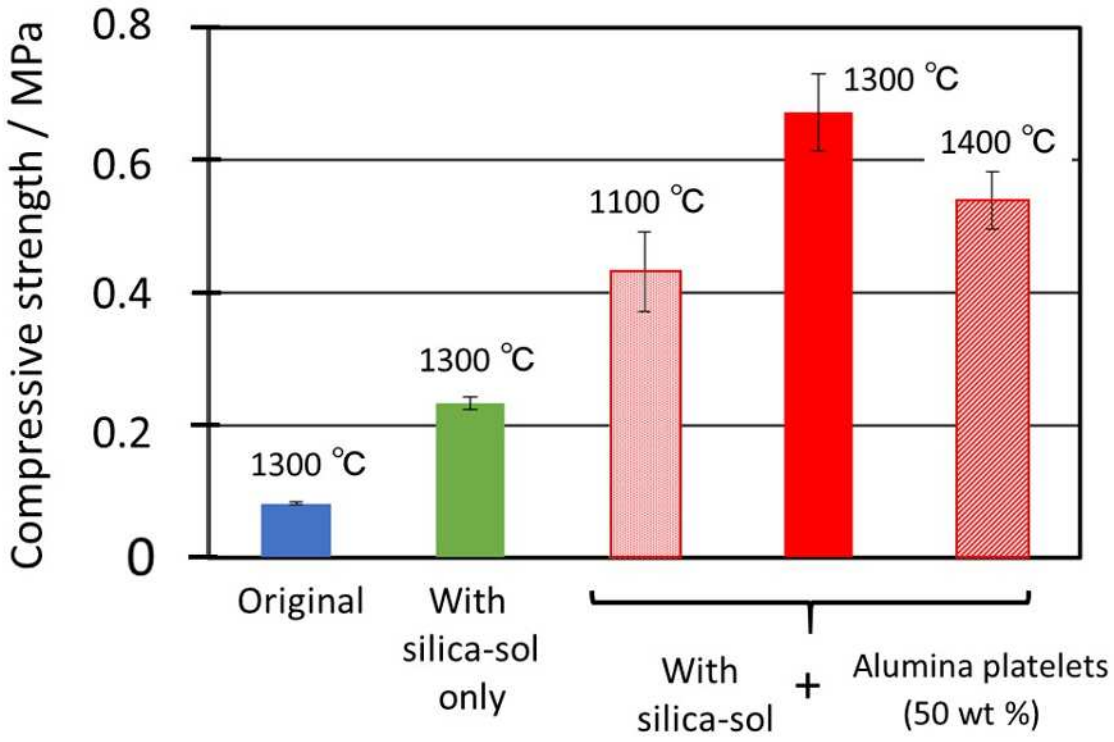
Compressive strength / MPa
0.8
0.6
0.4
0.2
0
1300 ℃
1300 ℃
1100 ℃
1300 ℃
1400 ℃
Original
With silica-sol only
With silica-sol
+
Alumina platelets (50 wt %)

Figure 7

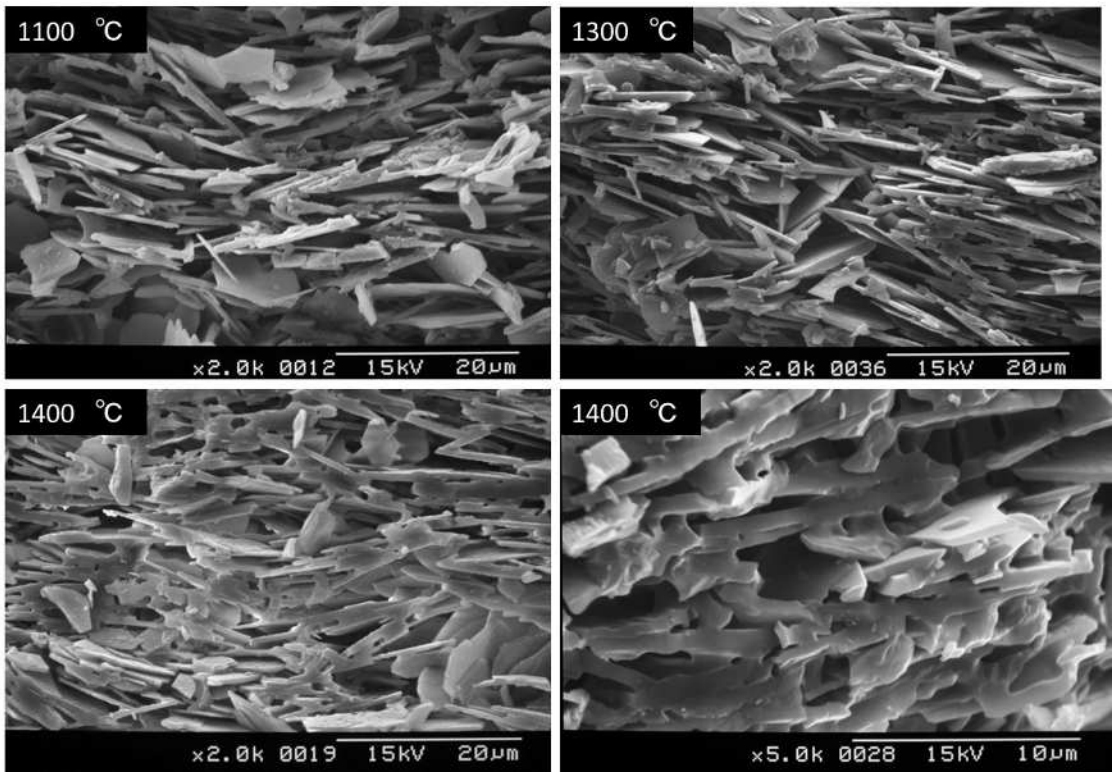
1100 ℃
×2.0k 0012 15kV 20μm
1300 ℃
×2.0k 0036 15kV 20μm
1400 ℃
×2.0k 0019 15kV 20μm
1400 ℃
×5.0k 0028 15kV 10μm

Figure 8

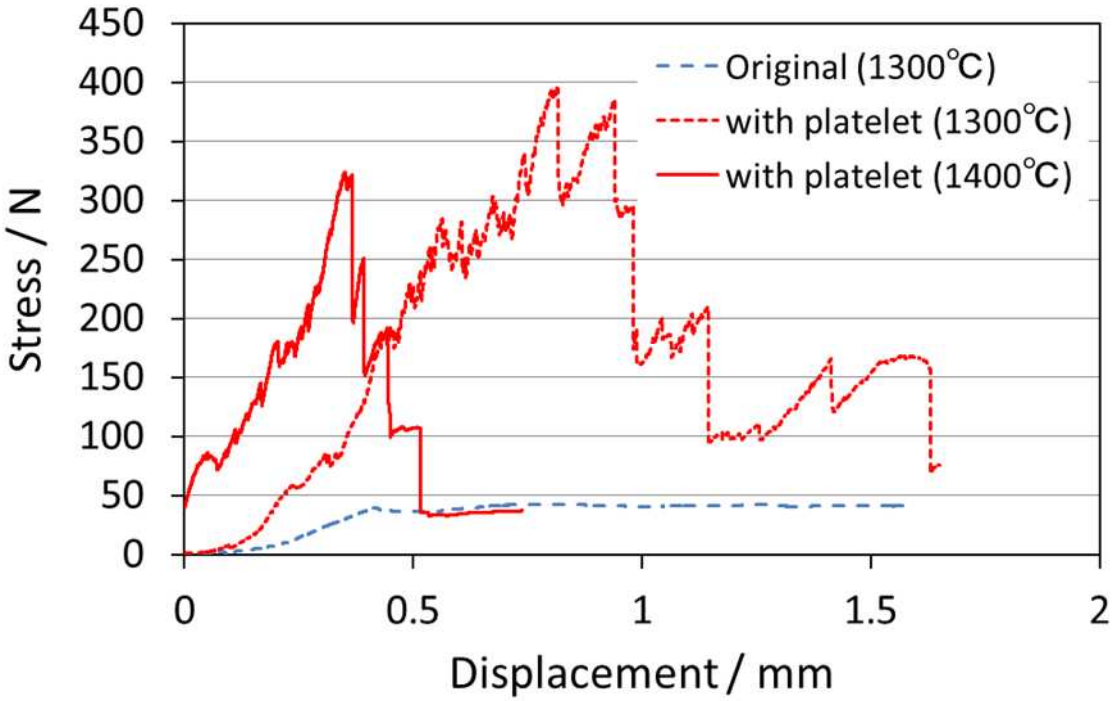
Original (1300℃)
with platelet (1300℃)
with platelet (1400℃)
Stress / N
Displacement / mm
0
50
100
150
200
250
300
350
400
450
0
0.5
1
1.5
2

Figure 9

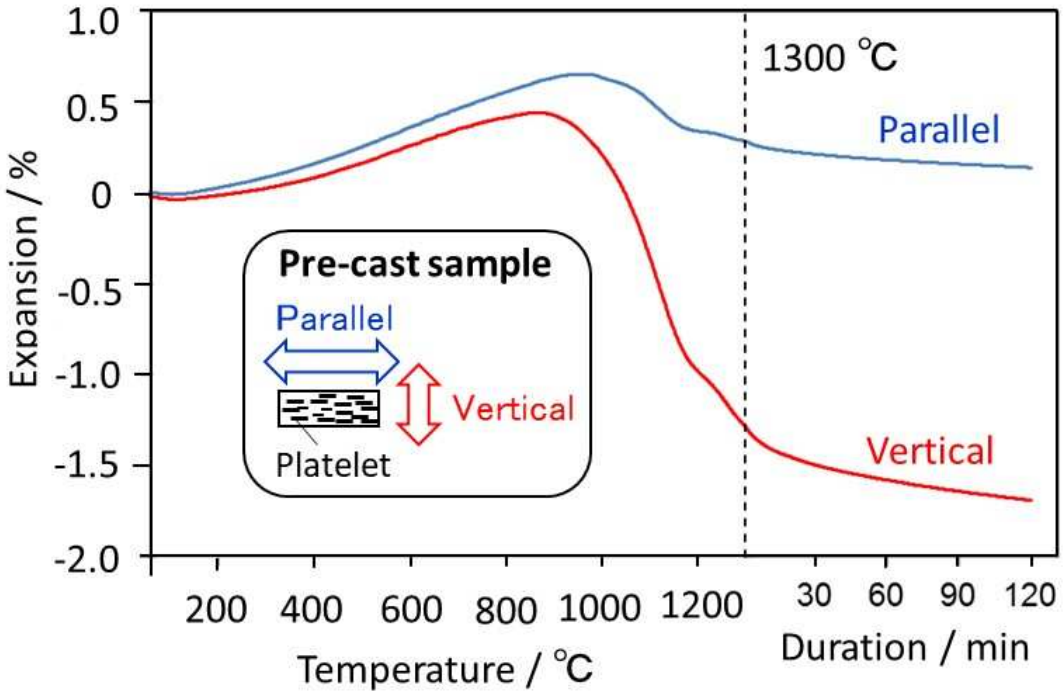
1.0
0.5
0
-0.5
-1.0
-1.5
-2.0
Expansion / %
1300 ℃
Parallel
Vertical
Pre-cast sample
Parallel
Vertical
Platelet
200
400
600
800
1000
1200
Temperature / ℃
30
60
90
120
Duration / min

Figure 10

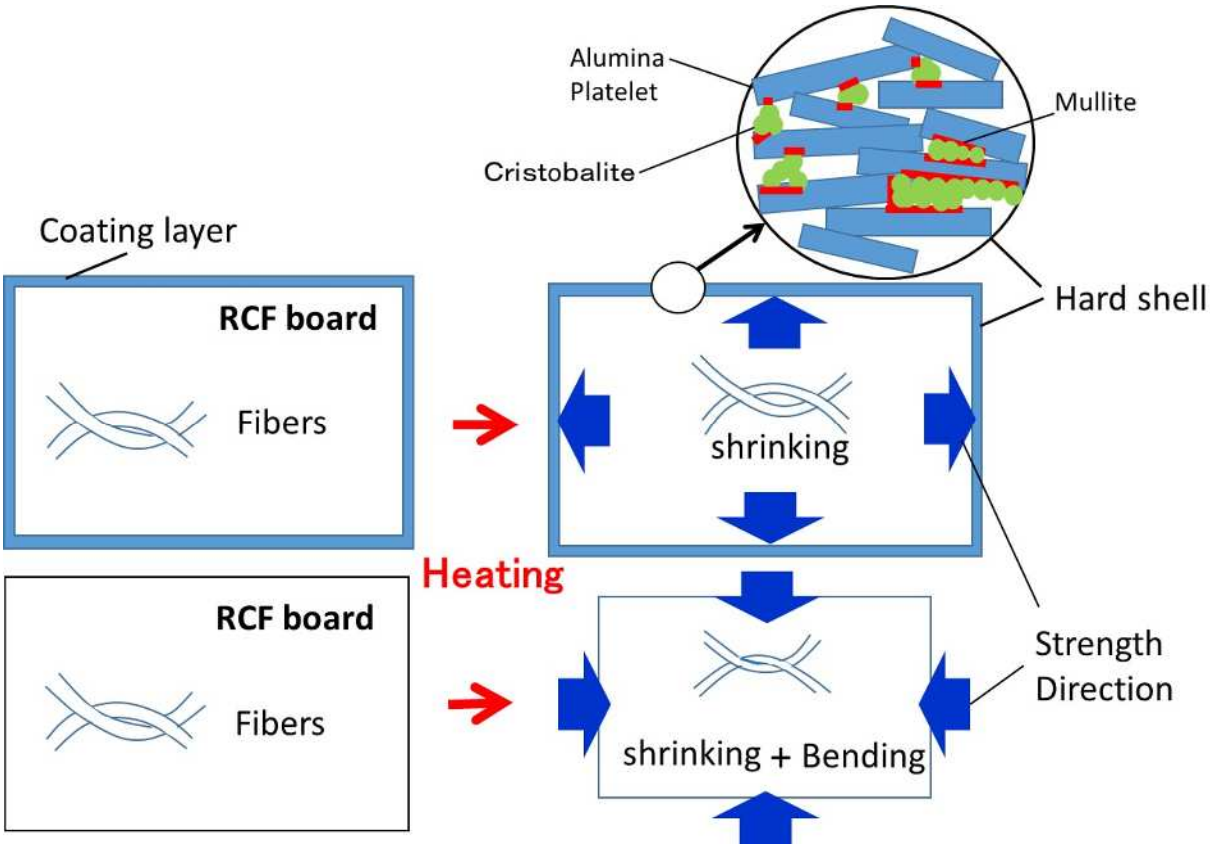
Alumina
Platelet
Mullite
Cristobalite
Coating layer
RCF board
Fibers
Hard shell
shrinking
Heating
RCF board
Fibers
Strength
Direction
shrinking + Bending

Table 1

	Composition (mass%)
Ignition loss	5
Al_2O_3	44
SiO_2	56

Table 2

Silica content	40 mass%
Na_2O content	< 0.5 mass%
pH	8.5-9.5
Mean particle size	18 nm
Density	1.3 g/cm^3

Table 3

	alumina (size: 0.5 μm)	alumina (size: 1 μm)	alumina (size: 5 μm)	alumina (platelets)
Al_2O_3 (mass%)	≥ 99.99	99.7	99.7	99.3
SiO_2 (mass%)	0.0030	0.08	0.02	0.06
Na_2O (mass%)	0.0004	0.15	0.26	0.17
Fe_2O_3 (mass%)	0.0003	0.02	0.01	0.02
Median particle size (μm)	0.45	0.96	4.5	8.8

*Aspect ratio: 25-30